NMR studies on ligand exchange at $[IrH_2Cl(CO)(PPh_3)_2]$ and $[IrH_2Cl(PPh_3)_3]$ by *para*-hydrogen induced polarisation

Christopher J. Sleigh,[a] Simon B. Duckett*[a] and Barbara A. Messerle[b]

[a] *Department of Chemistry, University of York, Heslington, York, UK YO1 5DD*
[b] *School of Chemistry, University of Sydney, Sydney, NSW 2006, Australia*

Enhancement of NMR signals by *para*-hydrogen induced polarisation allows the rapid characterisation of $[IrH_2Cl(CO)(PPh_3)_2]$ and $[IrH_2Cl(PPh_3)_3]$: these complexes undergo ligand exchange *via* a 16-electron complex, $[IrH_2Cl(PPh_3)_2]$, which has a square-based pyramidal structure.

Although the relatively small Boltzmann excess of nuclei available for detection makes NMR spectroscopy intrinsically insensitive, the size of the detectable signal can be enhanced by achieving a non-Boltzmann spin population. A notably successful way of doing so is to use *para*-hydrogen (p-H_2) which [1,2] has been shown to facilitate the observation of materials that are found only in low concentrations. In particular, intermediates in catalytic hydrogenation reactions such as $[Rh(H)_2Cl(PPh_3)_2(alkene)]$, species in minor reaction pathways such as $[RhH_2(PPh_3)_2Cl_2Rh(PPh_3)(CO)]$ and minor constituents in equilibria, for example all-*cis*-$[Ru(PMe_3)_2(CO)_2(H)_2]$, have been examined using this approach.[3]

The reaction chemistry forming the basis of the present study is the well known oxidative addition of H_2 to $[IrCl(CO)(PPh_3)_2]$ **1**, which yields p-H_2 active $[IrH_2Cl(CO)(PPh_3)_2]$ **2**, *via* a concerted pathway. In the presence of PPh_3, **2** undergoes CO loss to form p-H_2 active $[IrH_2Cl(PPh_3)_3]$ **3** (Scheme 1).[4] We now describe how the sensitivity gain provided by p-H_2 allows the rapid and unambiguous structural assignment of **2** and **3**. In particular, we show how two-dimensional homo- and heteronuclear NMR methods can be used to make spin system assignments, probe spatial arrangements of ligands and monitor ligand exchange. These experiments were achieved at extraordinary speed, using low concentrations of **1** (< 1 mmol dm^{-3}), and establish the viability of p-H_2 enhanced NMR spectroscopy as a mechanistic probe.

When a 1 mmol dm^{-3} solution of **1** in $[^2H_8]$toluene containing a 45-fold excess of PPh_3 and under 3 atm of p-H_2 is warmed to 343 K and monitored by ^1H NMR spectroscopy enhanced resonances are detected for the hydride ligands of **2** and **3**. The time-averaged spin state of the starting *para*-hydrogen derived magnetization is longitudinal two spin order and can be represented by the product operator formalism[5] $I_{Az}I_{Bz}$ (A and B represent the two protons of dihydrogen).[6] On application of a hard pulse of flip angle ϕ about the x axis, the magnetization becomes: $\frac{1}{2}\{I_{Az}I_{Bz}\cos^2\phi - I_{Az}I_{By}\sin2\phi - I_{Ay}I_{Bz}\sin2\phi + I_{Ay}I_{By}\sin^2\phi\}$ and the observable signal arises from the I_zI_y terms. Both sets of hydride resonances for **2** and **3** are therefore antiphase with respect to J_{AB}, the coupling constant between the two hydrogen nuclei, and yield optimal signal intensity when ϕ is $\pi/4$. From this point onwards the effect of radiofrequency pulses on the evolving magnetization can be predicted in the normal way.

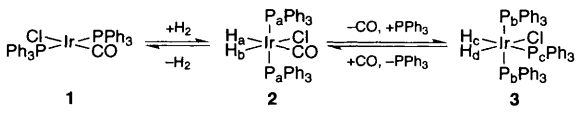

1 **2** **3**

Scheme 1

The heteronuclear experiments described in this work employ the heteronuclear single quantum correlation (HSQC)[7] pulse sequence, where the polarization transfer from protons to heteronuclei is achieved *via* an INEPT protocol.[8] The INEPT sequence (H–X) has been used extensively to transfer polarization from p-H_2 enhanced proton signals to coupled heteronuclei.[4,9]

In a typical HSQC[7] spectrum, cross-peaks connecting the resonances of the phosphorus nuclei of **2** and **3** to the resonances of their hydride coupling partners are visible [Fig 1(*a*)]. In order to assign resonances for protons that were not directly coupled to the hydride ligands, but also coupled to ^{31}P, magnetization was relayed across the coupling network $^1H \rightarrow {}^{31}P \rightarrow {}^1H$.[6] Using this approach resonances for the *ortho*-phenyl protons of the phosphines in **2** and **3** are now enhanced and easily located [Fig. 1(*b*)].† Coupled pairs of hydrides can also be assigned quickly because the antiphase magnetization generated after the first $\pi/4$ pulse is ideal for cross-peak formation in a COSY experiment [Fig. 1(*c*)]. At the onset of the experiment the intensities of the COSY cross-peaks connecting enhanced proton pairs far outweighed those of their diagonal counterparts [Fig. 1(*c*)].

Dipolar relaxation and the NOESY experiment have been widely utilized to obtain information about internuclear distances and exchange processes.[10] As the three-pulse NOESY experiment relies on the creation of z magnetization with the second pi pulse the starting antiphase magnetization was refocused, for a period of $\frac{1}{2}J_{HH}$, prior to the variable delay. A series of NOESY spectra with mixing times (τ_m) ranging between 100 ms and 1.6 s, and total acquisition times between 10 and 20 min were collected (Fig. 2). Cross-peaks were only observed as a result of magnetization transfer from p-H_2 enhanced resonances. Both positive (due to chemical exchange) and negative cross-peaks (due to NOE enhancements) were observed and their intensities increased with mixing time until relaxation effects dominated (Table 1). For example, at 343 K negative cross-peaks were found to interconnect the hydride

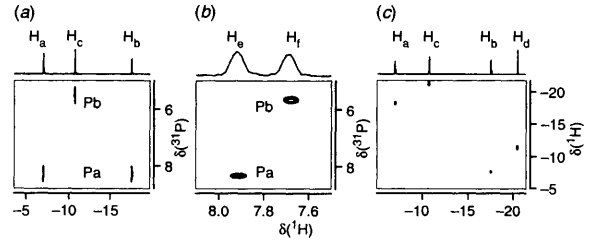

Fig. 1 Selected cross-peaks and projections from 2D correlation spectra obtained for $[IrH_2Cl(CO)(PPh_3)_2]$ **2** and $[IrH_2Cl(PPh_3)_3]$ **3** using modified pulse sequences (complexes generated by warming **1** with excess PPh_3 in C_6D_6 under p-H_2). (*a*) ^{31}P–^1H HSQC correlation spectrum (positive contours), cross-peaks connect P_a and P_b to their hydride coupling partners (343 K). (*b*) Inverse relayed ^{31}P,^1H shift correlation spectrum showing cross-peaks (absolute value display) connecting P_a and P_b to their *ortho*-phenyl protons (333 K). (*c*) ^1H–^1H correlation spectrum showing the cross-peaks (absolute value display) connecting H_a and H_b in **2**, and H_c and H_d in **3** (343 K).

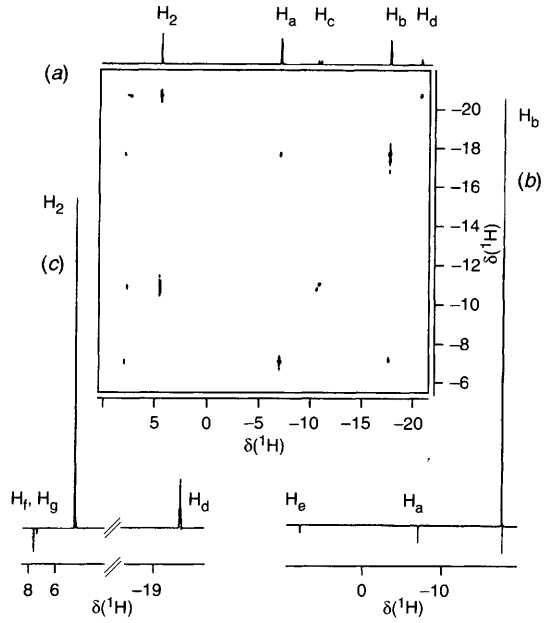

Fig. 2 ^1H–^1H NOESY spectrum of $[IrH_2Cl(CO)(PPh_3)_2]$ and $[IrH_2Cl(PPh_3)_3]$ obtained with *p*-H_2 in C_6D_6 at 343 K using a mixing time of 300 ms, and a 45-fold excess of PPh_3 relative to **1**. (*a*) Section of NOESY spectrum illustrating peaks due to H_a and H_b in **2**, H_c and H_d in **3**, and the cross-peaks that connect them (positive/negative contours). (*b*) Row extracted from the data displayed in (*a*) containing the diagonal element for H_b of **2**, NOE effects between H_b and H_a, and the *ortho*-phenyl protons H_g of the phosphine give rise to the negative peaks. (*c*) Row extracted from the data displayed in (*a*) containing the diagonal element for H_d of **3**, NOE interactions between H_d and H_f attached to P_b, and H_g attached to P_c give rise to the negative signals, exchange peaks correspond with free H_2 and H_c.

Table 1 % Cross-signal intensities extracted from NOESY spectra for free H_2 and H_c of **3** relative to the diagonal peak H_d as a function of mixing time (343 K, 45-fold excess of PPh_3 relative to **1**)

Mixing time/ms	Free H_2	H_c	*ortho*-Phenyl protons of P_b
100	11	13	−4
300	84	72	−19
500	134	76	−53
1600	536	100	−419

ligands of **2**, and also to interconnect the hydride ligands with the *ortho*-phenyl protons of the bound phosphine [Fig. 2(*b*)]. Only in the corresponding NOESY spectrum at 363 K do additional positive cross-peaks connect the hydride resonances of **2** to those of free H_2.

Negative cross-peaks were also observed in these experiments between (*i*) the resonances of H_d and the *ortho*-phenyl proton resonances H_f and H_g of P_b and P_c in **3** respectively [Fig. 2(*c*)], and (*ii*) the resonances due to H_o and the *ortho*-phenyl protons H_e of P_b (Table 1). These through-space interactions confirm that H_c is *trans* to P_c and *cis* to P_b and illustrate that *p*-H_2 enables the rapid probing of ligand arrangements.

For **3**, the hydride resonances, H_c and H_d, are connected by exchange peaks to themselves and the resonance for free H_2 at 343 K [Fig. 2(*c*), Table 1]. For a given mixing time, increasing the concentration of free PPh_3 first dramatically increases the intensity of the intramolecular exchange peaks between H_c and H_d, while concurrently reducing intermolecular exchange peaks to free H_2. However, at even higher PPh_3 concentrations (>500-fold excess relative to **1**), the intensity of the self-exchange peaks between H_c and H_d is diminished.

These results suggest that **3** undergoes exchange of PPh_3 *trans* to hydride to form the 16 electron complex,

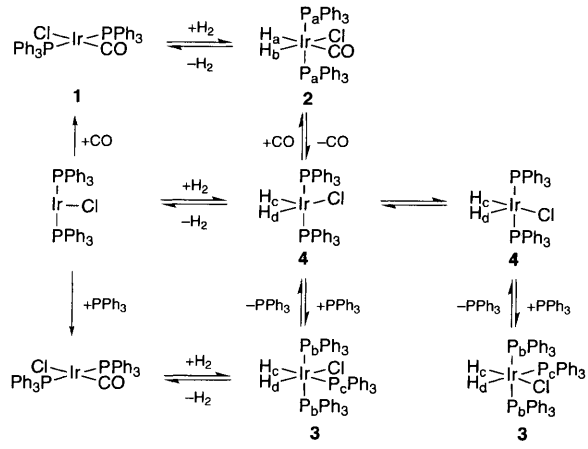

Scheme 2 (Both isomers of **4** can eliminate hydrogen)

$[IrH_2Cl(PPh_3)_2]$ **4**. Complex **4** can then either recoordinate PPh_3 to reform **3**, or reductively eliminate H_2. The observation that the latter process is suppressed by the addition of PPh_3 is consistent with a reduced lifetime for **4**. Additionally, the observed reduction in the rate of interconversion of H_c and H_d at higher PPh_3 concentrations requires that the hydride ligands of **4** retain a distinct identity (Scheme 2). This suggests that $[IrH_2Cl(PPh_3)_2]$ must adopt a square-pyramidal geometry in solution with chemically distinct hydrides; the phosphine dependence arises from the step in H_d and H_c exchange identities. This result contrasts with the congener $[RhH_2Cl(PPh_3)_2]$[11] which has equivalent hydrides and C_{2v} symmetry: $[Ir(H)_2Cl(P^tBu_2Ph)_2]$, however, has been shown to contain inequivalent hydride ligands.[12]

Financial support of this work from the SCI and EPSRC (C. S.), the University of York, the Royal Society and the Australian Research Council (B. A. M.), and a generous loan of iridium trichloride from Johnson Matthey are gratefully acknowledged.

Footnote

† *Selected spectroscopic data* at 343 K for **2** and **3** in $C_6D_5CD_3$ at 500.13 MHz (^1H) and 202.45 MHz (^{31}P). **2**: ^1H; δ 7.91 (H_c, *ortho*-phenyl proton of P_a), δ −7.02 [H_a, $J(P_aH)$ 18.8, J(HH) −5.7 Hz], −17.6 [H_b, $J(P_aH)$ 13.7, J(HH) −5.7 Hz]. ^{31}P; δ 8.4 (P_a, s). **3**: ^1H; δ 7.67 (H_f, *ortho*-phenyl proton of P_b), 7.42 (H_g, *ortho*-phenyl proton of P_c), −10.8 [H_c, $J(P_bH)$ 20.6 $J(P_cH)$ 130.6, J(HH) −7 Hz], −20.6 [H_d, $J(P_bH)$ 14.3, $J(P_cH)$ 14.3, J(HH) −7 Hz]. ^{31}P; δ −2.8 [P_c, t, J(PP) 26 Hz], 5.7 [P_b, d, J(PP) 26 Hz].

References

1 R. Eisenberg, *Acc. Chem. Res.*, 1991, **24**, 110.
2 C. R. Bowers and D. P. Weitekamp, *J. Am. Chem. Soc.*, 1987, **109**, 5541.
3 S. B. Duckett, C. L. Newell and R. Eisenberg, *J. Am. Chem. Soc.*, 1994, **116**, 10548. S. B. Duckett and R. Eisenberg, *J. Am. Chem. Soc.*, 1993, **115**, 5292. S. B. Duckett, R. J. Mawby and M. G. Partridge, *Chem. Commun.*, 1996, 383.
4 S. B. Duckett, C. L. Newell and R. Eisenberg, *J. Am. Chem. Soc.*, 1993, **115**, 1156. S. B. Duckett, R. Eisenberg and A. S. Goldman, *J. Chem. Soc., Chem. Commun.*, 1993, 1185.
5 O. W. Sorensen, G. W. Eich, M. H. Levitt, G. Bodenhausen and R. R. Ernst, *Prog. Nucl. Magn. Reson. Spectrosc.*, 1983, **16**, 163.
6 C. R. Bowers and D. P. Weitekamp, *Phys. Rev. Lett.*, 1986, **57**, 2645.
7 G. Bodenhausen and D. J. Ruben, *J. Chem. Phys. Lett.*, 1980, **69**, 185.
8 G. A. Morris and R. Freeman, *J. Am. Chem. Soc.*, 1979, **101**, 760.
9 J. Barkemeyer, M. Haake and J. Bargon, *J. Am. Chem. Soc.*, 1995, **117**, 2927.
10 H. Kessler, M. Gehrke and C. Griesinger, *Angew. Chem., Int. Ed. Engl.*, 1988, **27**, 490.
11 J. M. Brown, P. L. Evans and A. R. Lucy, *J. Chem. Soc., Perkin Trans. 2*, 1987, 1589.
12 B. E. Hauger, D. Gusev and K. G. Caulton, *J. Am. Chem. Soc.*, 1994, **116**, 208.

Received, 20th August 1996; Com. 6/05803E